The Effect of Real-Time Radar Transmitter Amplifier Impedance Tuning on Range and Doppler Detection Accuracy

Austin Egbert[1], Kyle Gallagher[2], Benjamin Kirk[3], Mark Kozy[4], Anthony Martone[2], Charles Baylis[1], Edward Viveiros[2], Robert J. Marks II[1]
[1]Baylor University, Waco, TX, USA
[2]Army Research Laboratory, Adelphi, MD, USA
[3]Pennsylvania State University, State College, PA, USA
[4]Virgina Polytechnic Institute and State University, Blacksburg, VA, USA

***Abstract*—Radar transmitter power amplifiers with tunable matching networks, designed to allow real-time spectrum flexibility, may require hundreds of milliseconds to reconfigure; which is typically a significantly longer duration than the coherent processing interval (CPI) of a radar. As such, it is desirable to perform accurate radar detection during the reconfiguration. The tuning operation, however, may affect the Doppler detection accuracy, due to the change in the tuner transmission phase during the measurement. Since Doppler error is proportional to the speed with which a mechanical tuning element is moved, fast tuners can cause significant impact on Doppler detection accuracy. Measurement results with a 90 W reconfigurable evanescent-mode cavity impedance tuner on the transmitter are presented for detection during reconfiguration, and approaches for ensuring accurate radar detection while reconfiguring are discussed.**

***Index Terms*—circuit optimization, cognitive radar, dynamic spectrum allocation, frequency agility, tunable circuit, power amplifiers.**

I. Introduction

With the advent of new high-power tunable circuitry, the concept of a tunable radar transmitter is now feasible for real-time spectrum sharing. Kingsley presents an adaptive amplifier module capable of real-time impedance tuning on the transmitter power amplifier covering a limited area of the Smith Chart [1], and Semnani [2] and Dockendorf [3] demonstrate a high-power tuner with even greater Smith Chart coverage and the capability to provide S-band frequency agility with up to 90 W of power handling. Because the time required for real-time tuning achievable by mechanical tuners is significantly longer than the pulse repetition interval (PRI) or coherent processing interval (CPI) of radars, it is desirable to perform detection during the tuning process. Zeidan discusses an approach to detect and correct transient phase shifts in RF receiver chains [4]. Velijanovski presents the effect of Doppler due to relative motion of transmitter to receiver on signal to noise ratio in a reconfigurable filter [5]. Tunability of devices has been exploited for phase-shift related operations such as beamforming using micro-electrical mechanical systems (MEMS) tunable phase shifters [6]. In addition, unwanted Doppler shifts have been noticed in acousto-optic filter design, as presented by Boyd [7]. We demonstrate how real-time impedance tuning in reconfigurable radar transmitters can impact range and Doppler detection accuracy.

II. Theory

The measurements provided by a radar system are ascertained by comparison of a received time-delayed and frequency shifted echo signal from a radar target with the transmitted signal. The time delay gives the range of the target, while the frequency shift (*aka* the Doppler shift) denotes both the magnitude and sign (direction) of the velocity of the target. This Doppler shift, is defined by the change in phase of the received signal as follows:

$$f_D = \frac{1}{2\pi}\frac{d\emptyset(t)}{dt}. \quad (1)$$

Because reconfiguration adjusts the tuner's S_{21}, an artificial Doppler frequency shift, based on tuner movement, may result if radar measurements are conducted while a tuner is in the process of reconfiguration.

III. Experimental Results

The evanescent-mode cavity tuner [2] system used for our experiments is shown in Fig. 1. Fig. 2 shows power-added efficiency (PAE) load-pull results at 3.55 GHz using this tuner with a Microwave Technologies MWT-173 field-effect transistor (FET) based on cavity position numbers n_1 and n_2, which reconfigure the power amplifier load impedance around the Smith Chart. Maximum PAE occurs near $(n_1, n_2) = (6900, 7000)$.

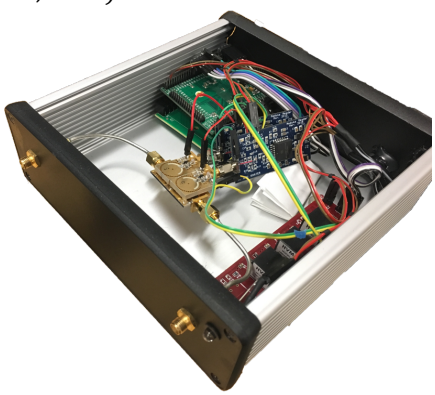

Fig. 1. Evanescent-mode cavity tuner with piezo actuators [2]

978-1-7281-1803-1/19/$31.00 ©2019 IEEE

In the first experiment, the tuner was set to a position of $(n_1, n_2) = (6000, 6000)$, and the range and Doppler of a simulated target were measured. 500 acquisitions of 8192 samples were collected at 10 MS/s using a Hamming windowed chirp waveform with 3 MHz bandwidth centered at 3.55 GHz with a 50 % duty cycle. The simulated target is located approximately 49.8 km downrange and exhibits a Doppler shift on the order of 49 Hz. Transmission through the tuner, both with the tuner stationary and moving, is part of the measurement. Fig. 3 shows four range/Doppler detections, each with four sets of 500 acquisitions: (1) tuner stationary at (6000, 6000), (2) tuner stationary at (7200, 7200), (3) tuner moving from (6000, 6000) to (7200, 7200), and (4) tuner moving from (7200, 7200) to (6000, 6000). These tuner positions are chosen to demonstrate the most significant transition based on Fig. 2. For the two stationary settings 1 and 2, the detected range and Doppler are the same and correspond to the actual range and Doppler of the target. However, in setting 3, when the tuner is moving from (6000, 6000) to (7200, 7200), an apparent Doppler shift of -0.29 Hz is visible relative to the detected Doppler under stationary tuner conditions, a left shift in Fig. 3. Additionally, in setting 4, when the tuner is moved from (7200, 7200) to (6000, 6000), an apparent relative Doppler shift of +0.29 Hz (right shift) is observed. In settings 3 and 4, the changing phase of the tuner's S_{21} causes the artificial Doppler shift, based on the speed of the tuner movement from equation (1). While for this tuner, the $\pm$ 0.29 Hz errors would likely translate to approximately 3 cm/s of velocity error, faster reconfiguration times in next-generation tuners under development are expected to result in larger Doppler shifts on the order of 15 Hz, for a velocity error near 1.5 m/s (3.4 miles/hour).

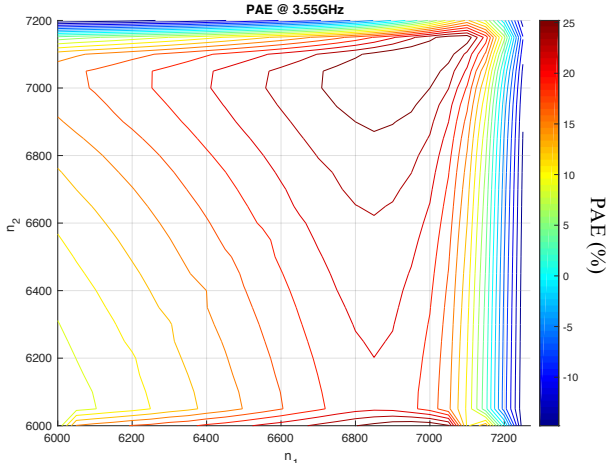

Fig. 2. MWT-173 FET power-added efficiency (PAE) contours for variations of cavity position numbers (n_1, n_2) at 3.55 GHz

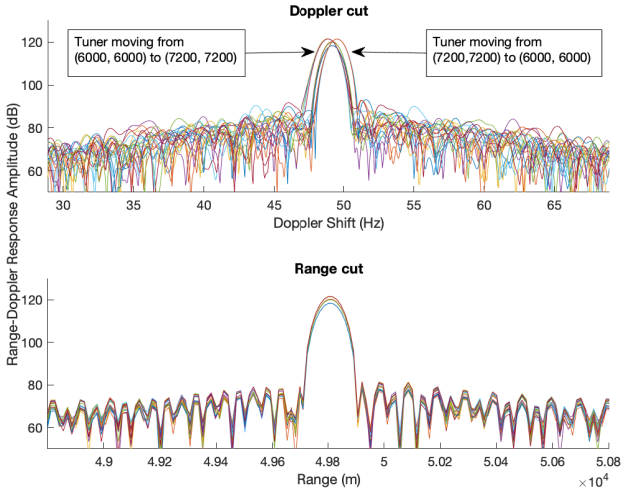

Fig. 3. Doppler and range detection results from measurements with simulated radar target: (1) tuner stationary at (6000, 6000) (blue), (2) tuner stationary at (7200, 7200) (green), (3) tuner moving from (6000, 6000) to (7200, 7200) (red), and (4) tuner moving from (7200, 7200) to (6000, 6000) (yellow)

The change in S_{21} phase versus time was measured, for an identical second tuner located at a separate remote facility, while it was tuned across the entire range of both tuner actuators from (6000, 6000) to (7500, 7500). Fig. 4 shows the phase of S_{21} versus time for both upward and downward changes in the cavity positions. Using a sample-by-sample estimation of the derivative in Eq. (1), the predicted artificial frequency shift at the nth time sample can be computed as follows:

$$\Delta f[n] = \frac{\emptyset[n+1] - \emptyset[n]}{\Delta t} \times \frac{1}{360°}, \qquad (2)$$

where $\emptyset[n]$ and $\emptyset[n+1]$ are the phase values, in degrees, at the nth and $(n+1)$th samples, respectively, and Δt is the time between samples. Based on this approach, the expected instantaneous detected Doppler shifts are plotted versus time in Fig. 5. The initially large-amplitude activity observed in the interval 0.4 s < t < 0.6 s is attributed to the start-up of tuner movement. During the interval 1 s < t < 2 s (in each case) the tuner performs its movement, and the expected Doppler frequency shift ranges from 0 < f < 4 Hz. The maximum value of this shift is much larger than the approximately $\pm$ 0.29 Hz observed in Fig. 3. This is because the range-Doppler processing averages the measured instantaneous frequency shift over all acquisitions. For these measurements, the acquisition roughly overlaps the 0.5 s < t < 1.75 s interval of Fig. 4, resulting in an observed phase shift of nearly 130 degrees over 1.25 s. This would correspond with a uniform Doppler shift of approximately 0.36 cycles/1.25 s = 0.288 Hz, corresponding with the $\pm$ 0.29 Hz shift of Fig. 3.

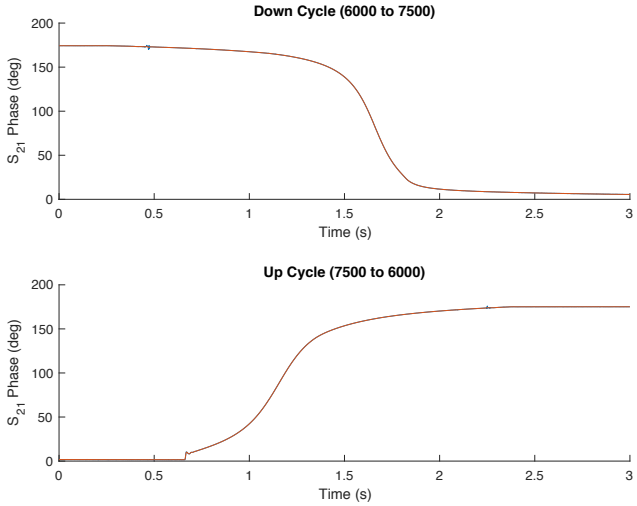

Fig. 4. Tuner S_{21} phase versus time in tuning from (7500, 7500) to (6000, 6000) (top) and from (6000, 6000) to (7500, 7500) (bottom)

These measurement results are confirmed by using a second measurement setup where two waveforms with identical frequency are generated, with one of the waveforms going through the tuner, and then mixed together as shown in Fig. 6. When the tuner is moved, the S_{21} phase change causes the waveform to change phase by 180 degrees over the tuning time, and a partial sinusoid, generated by the varying relative phase of the mixer inputs and corresponding to the artificial Doppler shift, will appear at the output of the mixer until the tuner has settled at its new state, and the output takes on a new amplitude based on the new relative phase of the mixer inputs. Fig. 7 shows the mixer output during tuner movements in both directions: from (6000, 6000) to (7500, 7500) and then reversed. The calculation of the instantaneous frequency at the nth sample, $f[n]$, can be approximated by a forward difference as follows:

$$f[n] = \frac{1}{2\pi} \frac{\cos^{-1}\left(\frac{1}{A}y[n+1]\right) - \cos^{-1}\left(\frac{1}{A}y[n]\right)}{\Delta t}, \quad (3)$$

where $y[n]$ is the nth sample of the measured mixer output, A is the amplitude of the assumed cosine waveform, and Δt is the time between samples. Fig. 8 shows good correspondence between instantaneous frequency shift estimations from this down-conversion setup and Vector Network Analyzer (VNA) measurements.

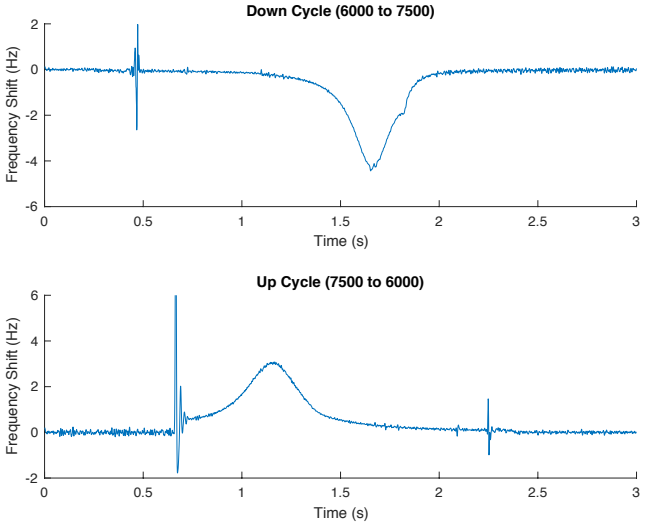

Fig. 5. Calculated estimated Doppler frequency shift versus time in tuning from (7500, 7500) to (6000, 6000) (top) and from (6000, 6000) to (7500, 7500) (bottom)

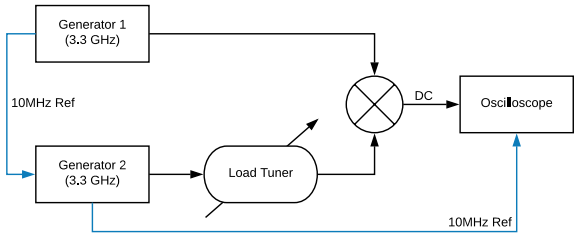

Fig. 6. Down-conversion measurement setup for frequency shift

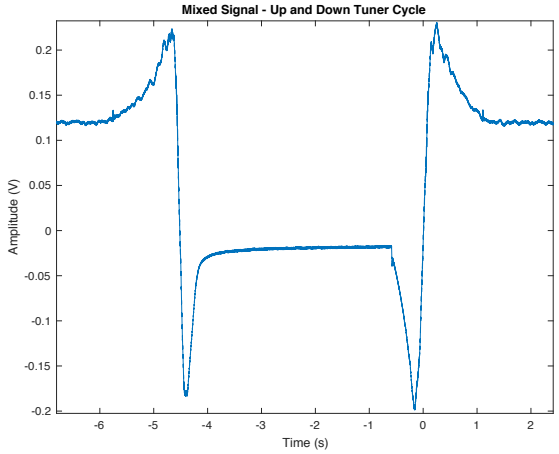

Fig. 7. Oscilloscope-measured signal for tuner transitions from (6000, 6000) to (7500, 7500) and reversed from (7500, 7500) to (6000, 6000)

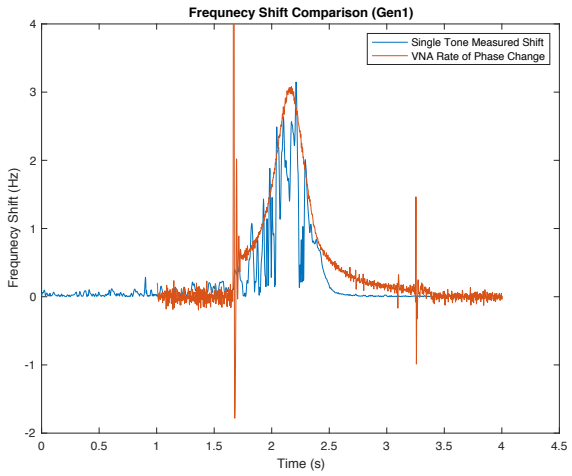

Fig. 8. Instantaneous frequency shift measurements from the Vector Network Analyzer (red) and down-conversion (blue) measurement setups

VI. Conclusions

Investigation of the effects of impedance tuning on radar detection shows that an artificial Doppler shift results from obtaining target data during tuner motion. The amount of the Doppler shift can be estimated by dividing the difference in the phase of S_{21} at the start and end tuner settings by the number of seconds required for the transition. While the Doppler shift for this first-generation, slow-moving impedance tuner was relatively small, it is expected that faster, next-generation impedance tuners will result in greater Doppler errors. To solve this issue, it is recommended that a measurement of the transmitter *output* waveform be used in the matched filtering at the receiver, or correction based on change in tuner S_{21} and tuning time be applied from a pre-characterization.

Acknowledgment

This work has been funded by the Army Research Laboratory (Grant No. W911NF-16-2-0054). The views and opinions expressed do not necessarily represent the opinions of the U.S. Government. The authors are grateful to John Clark of the Army Research Laboratory for assistance in development of this paper.

References

[1] N. Kingsley and J.R. Guerci, "Adaptive Amplifier Module Technique to Support Cognitive RF Architectures," 2014 IEEE Radar Conference, Cincinnati, Ohio, May 2014.

[2] A. Semnani, M. Abu Khater, Y.-C. Wu, and D. Peroulis, "An Electronically-Tunable High-Power Impedance Tuner with Integrated Closed-Loop Control," *IEEE Microwave and Wireless Components Letters*, Vol. 27, No. 8, August 2017, pp. 754-756.

[3] S. Rezayat, C. Kappelmann, Z. Hays, L. Hays, C. Baylis, E. Viveiros, A. Semnani, and D. Peroulis, "Real-Time Frequency-Agile Circuit Reconfiguration for S-Band Radar Using a High-Power Tunable Resonant Cavity Matching Network," 2018 IEEE MTT-S International Microwave Symposium, Philadelphia, Pennsylvania, June 2018.

[4] M.A. Zeidan, G. Banerjee, and J.A. Abraham, "Asynchronous Measurement of Transient Phase-Shift Resulting From RF Receiver State-Change," *IEEE Transactions on Circuits and Systems*, Vol. 60, No. 10, October 2013, pp 2740-2751.

[5] R. Velijanovski, J. Singh, and M. Faulkner, "Design and Implementation of Reconfigurable Filter," *Electronics Letters*, Vol. 39, No. 10, May 2003, pp. 813-814.

[6] K. Van Caekenberghe, "RF MEMS on the Radar," *IEEE Microwave Magazine*, Vol. 10, No. 6, October 2006, pp. 99-116.

[7] G.D. Boyd and F. Heismann, "Tunable Acoustooptic Reflection Filters in $LiNbO_3$ Without a Doppler Shift," *Journal of Lightwave Technology*, Vol. 7, No. 4, April 1989, pp. 625-631.